Biochimica et Biophysica Acta, 545 (1979) 106—121

BBA 47588

LINEAR DICHROISM AND THE ORIENTATION OF REACTION CENTERS OF *RHODOPSEUDOMONAS SPHAEROIDES* IN DRIED GELATIN FILMS

CHARLES N. RAFFERTY and RODERICK K. CLAYTON

Division of Biological Sciences, Cornell University, Ithaca, NY 14853 (U.S.A.)

(Received April 10th, 1978)

Key words: Reaction center; Linear dichroism; Bacteriochlorophyll; Bacteriopheophytin; Bacterial photosynthesis; (Rhodopseudomonas sphaeroides)

Summary

Aqueous mixtures of reaction centers of *Rhodopseudomonas sphaeroides* and gelatin were dried to form thin films. Following hydration, these films were stretched as much as two to three times their original length. Polarized absorption spectra showing linear dichroism were obtained for both unstretched and stretched films, with the planes and stretching axes of the films mounted in various geometries relative to the electric vector of the measuring beam. These data were analyzed in terms of the following model: Reaction centers possess an axis of symmetry that is fixed in relation to the reaction center structure. In unstretched films this axis is confined to the film plane and oriented at random within the plane. In stretched films the symmetry axis is aligned with the direction of stretching. In both preparations reaction centers are distributed randomly with respect to rotation about the axis of symmetry. The data are consistent with this model when the analysis acknowledges less than perfect orientation. For perfect orientation in a stretched film the model predicts uniaxial symmetry about the axis of stretching. The approach to this condition was examined with films stretched to different extents. Extrapolation yielded dichroic ratios for the ideal case of perfect orientation, and allowed calculation of the angles between the axis of symmetry and the various optical transition dipoles in the reaction center. This treatment included the two absorption bands of the bacteriochlorophyll 'special pair' (photochemical electron donor) in the Q_x region, at 600 and 630 nm, which we were able to resolve in light minus dark difference spectra.

Introduction

In a previous report [1] we described the linear dichroism of reaction centers of *Rhodopseudomonas sphaeroides* when the reaction centers were oriented in dried gelatin films. We have continued this study with the ultimate goal of describing the interaction and arrangement in space of the component chromophores: four bacteriochlorophyll and two bacteriopheophytin molecules per reaction center [2,3]. When aqueous mixtures of gelatin and reaction centers of *Rp. sphaeroides* are dried to form thin films, the magnitudes of the visible and near infrared absorption bands of the reaction centers are dependent on the polarization of the measuring beam relative to the film plane. When dried films are partially hydrated, stretched, and redried, the absorbances depend on the polarization of light relative to the stretching axis [1].

Linear dichroism spectra and light minus dark difference spectra of reaction centers in oriented preparations (in films of chromatophores [4] and in gelatin films [1] have yielded conclusions about the assignment of various absorption bands to certain chromophores, especially the two bacteriochlorophyll molecules ('special pair') that participate in photochemical electron donation, and the two molecules of bacteriopheophytin. These studies gave evidence for exciton interaction: splitting of the Q_y transition of the special pair into bands near 810 and 860 nm. One result of the present study was the resolution of the corresponding Q_x transition into bands near 600 and 630 nm.

We describe here a more quantitative study of the linear dichroism of reaction centers in unstretched and stretched gelatin films. Our analysis of linear dichroism spectra in various ways is compatible with a simple model for the type and degree of orientation of reaction centers in these films. Using this model we compute the orientations of various optical transition dipoles relative to an axis of symmetry in the reaction center. In a subsequent communication, we will show how these data can be combined with photoselection data to yield the radial coordinates of transition moment orientation.

Materials and Methods

Carotenoidless mutant strain R-26 of *Rp. sphaeroides* was grown phototrophically by the method of Clayton [5]. Reaction centers were isolated as described by Clayton and Wang [6]. Dried gelatin films containing reaction centers were prepared as described by Rafferty and Clayton [1]. Absorption spectra were recorded with a Cary 14R Spectrophorometer fitted with Glan-Thompson polarizers in the measuring beams. Techniques of data acquisition and photo-excitation of samples are described by Vermeglio and Clayton [4]. Light-induced changes were measured with a splitbeam absorption spectrometer [7]. Actinic light was provided by a xenon flash lamp. A series of such measurements provided the data for constructing light minus dark difference spectra. All experiments were made at 20—25°C.

Derivation of equations

We shall derive equations that predict dichroic ratios for different geometries of the gelatin film in relation to the polarized measuring beam, using a specific model for the orientation of reaction centers in unstretched and stretched films. The usefulness of the model will be judged from the economy and accuracy with which various experimental data are accommodated. Our derivations were guided by reports of Cherry et al. [8] and Fraser [9].

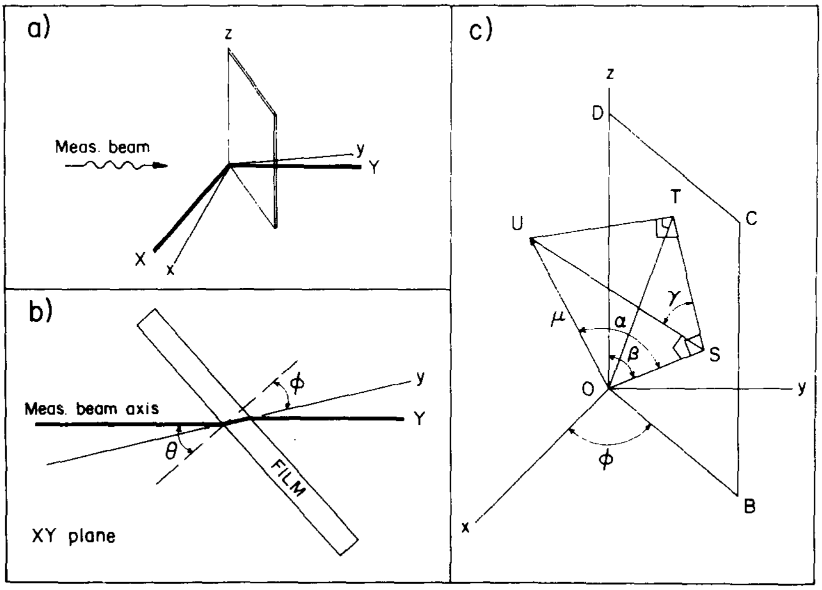

Fig. 1. The geometrical relationships between the measuring beam, a gelatin film containing reaction centers of *Rp. sphaeroides*, and a transition dipole fixed with respect to the film. Details in the text.

Basic geometry and statement of a model

Fig. 1a and 1b defines a coordinate system for the experimental arrangement of measuring beam and gelatin film. The Y axis is the axis of the measuring beam (horizontal); the X and Z axes are perpendicular to the measuring beam, horizontal and vertical respectively. The plane of the film is vertical and makes an angle θ with the XZ plane, so θ is the angle of incidence of the measuring beam on the film. Inside the film, the measuring beam makes an angle of refraction ϕ with the normal to the film; $\sin\theta = n \sin\phi$ where n is the refractive index of the gelatin film. Coordinates inside the film are specified by lower case: the y axis is the axis of the measuring beam inside the film and the x axis is normal to the y axis in the horizontal plane. The Z and z axes axes coincide. The xyz and XYZ systems are thus related by rotation about the Z axis through an angle $\theta - \phi$. For a vertically polarized measuring beam the electric vector is aligned with the Z axis; for horizontal polarization the electric vector is parallel to the x axis inside the film.

In Fig. 1c the plane of the film is shown by OBCD. The vector OS, in the film plane, represents a particular direction (axis of symmetry; see later) in a reaction center particle. The vector OU is a linear transition dipole moment in the same particle; its length is μ. OS makes an angle α with OU and β with the z axis. The length of OS is chosen so that SU is normal to OS. The angle between SU and ST is γ. Note that OSU, OST, OTU and STU are all right angles. The lengths of vectors in this diagram are:

$OU = \mu$ $\qquad$ $ST = \mu \sin\alpha \cos\gamma$

$OS = \mu \cos\alpha$ $\qquad$ $TU = \mu \sin\alpha \sin\gamma$

$SU = \mu \sin\alpha$

The components of OU projected on the z and x axes are $\mu_Z = \mu P$ and $\mu_x = \mu Q$, where

$$P = \cos\beta \cos\alpha + \sin\beta \cos\gamma \sin\alpha \qquad (1)$$

$$Q = \cos\phi \sin\beta \cos\alpha - \cos\phi \cos\beta \cos\gamma \sin\alpha + \sin\phi \sin\gamma \sin\alpha \qquad (2)$$

The absorbances of vertically and horizontally polarized light are denoted $A_V(\theta)$ and $A_H(\theta)$, respectively. Absorbance is related to transition dipole orientation in the following way:

$$A_V(\theta) = k\mu_z^2/K(\theta) = k\mu^2P^2/K(\theta) = A_\mu P^2/K(\theta) \qquad (3)$$

$$A_H(\theta) = k\mu_x^2/K(\theta) = k\mu^2Q^2/K(\theta) = A_\mu Q^2/K(\theta) \qquad (4)$$

where k is a constant and A_μ is the absorbance of light with the electric vector parallel to a linear transition dipole, for an arbitrary sample concentration. To compensate for changing path length when θ is altered, a factor $K(\theta)$ is introduced. $K(\theta)$ is defined as unity when $\theta = 0$; it is approximately * equal to $\cos\phi$. If the absorbance is measured with vertically polarized light and with θ set first at 0° and than at some value $\theta > 0$, Eqns. 1 and 3 give

$$A_V(0)/A_V(\theta)K(\theta) = 1 \qquad (5)$$

This equation is independent of the manner in which reaction centers are oriented in the film. It allows direct experimental evaluation of $K(\theta)$.

We now introduce three assumptions that define our model for the orientation of reaction centers in gelatin films: (1) The reaction centers (and their transition dipoles) are oriented randomly about an axis of symmetry that is fixed in the reaction center particle. This axis is OS in Fig. 1c. (2) The axis of symmetry lies in the plane of an unstretched film, with random orientation in that plane. (3) In a stretched film the same axis of symmetry is aligned with the direction of stretching. Later we shall relax the model to allow for imperfect adherence to the second and third assumptions.

Dichroic ratios for a stretched film

Our model states that in a stretched film the transition dipoles are distributed symmetrically about the OS axis; all values of γ have equal probability. We average $A_V(\theta)$ and $A_H(\theta)$ (Eqns. 3 and 4) over the domain of γ:

$$A_V(\theta) = [A_\mu/2\pi \cdot K(\theta)] \int_0^{2\pi} P^2\, d\gamma$$

$$A_H(\theta) = [A_\mu/2\pi \cdot K(\theta)] \int_0^{2\pi} Q^2\, d\gamma$$

---

* $K(\theta)$ would be exactly equal to $\cos\phi$ if the gelatin film were perfectly uniform in thickness. In practice the value of $K(\theta)$ was determined experimentally for the particular film being measured (see later). It did not differ from $\cos\phi$ by more than 2%.

giving

$$A_V(\theta) = (A_\mu/K(\theta))(\cos^2\beta \cos^2\alpha + \tfrac{1}{2} \sin^2\beta \sin^2\alpha) \quad (6)$$

$$A_H(\theta) = (A_\mu/K(\theta))(\cos^2\phi \sin^2\beta \cos^2\alpha + \tfrac{1}{2} \cos^2\phi \cos^2\beta \sin^2\alpha + \tfrac{1}{2} \sin^2\phi \sin^2\alpha) \quad (7)$$

When the film is mounted so that the stretching direction is vertical (parallel to the z axis), $\beta = 0°$ and

$$A_V(\theta) = (A_\mu/K(\theta)) \cos^2\alpha \quad (8)$$

$$A_H(\theta) = (A_\mu/2K(\theta)) \sin^2\alpha \quad (9)$$

The dichroic ratio is simply

$$A_V(\theta)/A_H(\theta) = 2 \cot^2\alpha \quad (10)$$

This equation has been derived by Fraser [9]. Axial symmetry about the axis of stretching is expressed by the fact that $A_V(\theta)/A_H(\theta)$ is independent of θ.

Another kind of dichroic ratio is obtained with the measuring beam polarized horizontally and the film turned to two values of θ, for example 0° and θ. Then for a stretched film with $\beta = 0$ (stretching direction vertical), Eqn. 9 yields

$$A_H(0)/A_H(\theta)K(\theta) = 1 \quad (11)$$

This again expresses axial symmetry about the axis of stretching.

Unstretched film

Our model states that in an unstretched film the axis of symmetry OS lies in the plane of the film with random orientation in that plane, so that all values of β, as well as all values of γ, are equally probable. We therefore average Eqns. 3 and 4 over the domains of both β and γ, obtaining

$$A_V(\theta) = (A_\mu/K(\theta))(\tfrac{1}{2} \cos^2\alpha + \tfrac{1}{4} \sin^2\alpha) \quad (12)$$

and

$$A_H(\theta) = (A_\mu/K(\theta))(\tfrac{1}{2} \cos^2\phi \cos^2\alpha + \tfrac{1}{4} \cos^2\phi \sin^2\alpha + \tfrac{1}{2} \sin^2\phi \sin^2\alpha) \quad (13)$$

These expressions yield

$$A_V(\theta)/A_H(\theta) = (\cos^2\alpha + \tfrac{1}{2} \sin^2\alpha)/(\cos^2\phi \cos^2\alpha + \tfrac{1}{2} \cos^2\phi \sin^2\alpha + \sin^2\phi \sin^2\alpha)$$
$$= A_H(0)/A_H(\theta)K(\theta) \quad (14)$$

Note that when $\theta = 0$, $\phi = 0$ and $A_V(0) = A_H(0)$.

Partial orientation

We do not expect that reaction centers in gelatin films are oriented perfectly as described by our model. One way to express imperfect orientation, suggested by Fraser [9], is to partition the population of reaction centers into a perfectly oriented fraction f and a residual fraction $(1 - f)$. The fraction f is described correctly by the foregoing equations. The absorbance in polarized light is then

$$A_V(\theta) = fA'_V(\theta) + A_{VR}(1 - f) \quad (15)$$

$$A_H(\theta) = fA'_H(\theta) + A_{HR}(1 - f) \quad (16)$$

where $A'_V(\theta)$ and $A'_H(\theta)$ are absorbances of the perfectly oriented fraction and A_{VR} and A_{HR} are those of the remaining fraction.

If the remaining fraction is oriented randomly,

$$A_{VR} = A_{HR} = A_\mu/3K(\theta) \tag{17}$$

Then the counterparts of Eqns. 10 and 11 (stretched film) become

$$A_V(\theta)/A_H(\theta) = [f_2 \cos^2\alpha + (1/3)(1-f_2)]/[\tfrac{1}{2} f_2 \sin^2\alpha + (1/3)(1-f_2)] \tag{18}$$

and

$$A_H(0)/A_H(\theta)K(\theta) = 1 \tag{19}$$

where f_2 is the value of f in a stretched film.

For an unstretched film, with the value of f denoted f_1, the counterparts of Eqns. 12—14 are

$$A_V(\theta) = [f_1 A_\mu/K(\theta)](\tfrac{1}{2}\cos^2\alpha + \tfrac{1}{4}\sin^2\alpha) + [A_\mu/3K(\theta)](1-f_1) \tag{20}$$

$$\begin{aligned} A_H(\theta) = {} & f_1[A_\mu/K(\theta)](\tfrac{1}{2}\cos^2\phi\cos^2\alpha + \tfrac{1}{4}\cos^2\phi\sin^2\alpha + \tfrac{1}{2}\sin^2\phi\sin^2\alpha) \\ & + [A_\mu/3K(\theta)](1-f_1) \end{aligned} \tag{21}$$

and

$$\begin{aligned} A_V(\theta)/A_H(\theta) = {} & [f_1(\tfrac{1}{2}\cos^2\alpha + \tfrac{1}{4}\sin^2\alpha) + (1/3)(1-f_1)]/[f_1(\tfrac{1}{2}\cos^2\phi\cos^2\alpha \\ & + \tfrac{1}{4}\cos^2\phi\sin^2\alpha + \tfrac{1}{2}\sin^2\phi\sin^2\alpha) + (1/3)(1-f_1)] \\ = {} & A_H(0)/A_H(\theta)K(\theta)\,. \end{aligned} \tag{22}$$

Finally we consider that in a stretched film the residual fraction, $1-f_2$, represents incomplete conversion from the 'unstretched' state to the idealized 'stretched' state. The residual fraction is then oriented not at random but as in an unstretched film. This is likely because the partial hydration prerequisite to stretching does not change the orientation of an unstretched film [1]. For this case we apply Eqns. 15 and 16, with f denoted f_2, but for A_{VR} and A_{HR} we use the values of $A_V(\theta)$ and $A_H(\theta)$ given by Eqns. 20 and 21. Now the counterpart of Eqn. 10 becomes

$$\begin{aligned} A_V(\theta)/A_H(\theta) = {} & [f_2\cos^2\alpha + f_1(1-f_2)(\tfrac{1}{2}\cos^2\alpha + \tfrac{1}{4}\sin^2\alpha) + (1/3)(1-f_1)(1-f_2)] \\ & \div [\tfrac{1}{2} f_2 \sin^2\alpha + f_1(1-f_2)(\tfrac{1}{2}\cos^2\phi\cos^2\alpha + \tfrac{1}{4}\cos^2\phi\sin^2\alpha + \tfrac{1}{2}\sin^2\phi\sin^2\alpha) \\ & + (1/3)(1-f_1)(1-f_2)] \end{aligned} \tag{23}$$

Note that although $A_V(\theta)/A_H(\theta)$ is independent of θ in Eqns. 10 and 18, it depends on ϕ and hence on θ in Eqn. 23.

Results

Polarized absorption by reaction centers in unstretched and stretched gelatin films

Fig. 2 shows the polarized absorption spectra and the corresponding linear dichroism spectrum of reaction centers in an unstretched gelatin film. Referring to Fig. 1, the film plane was vertical and θ was set at 60°. The corresponding

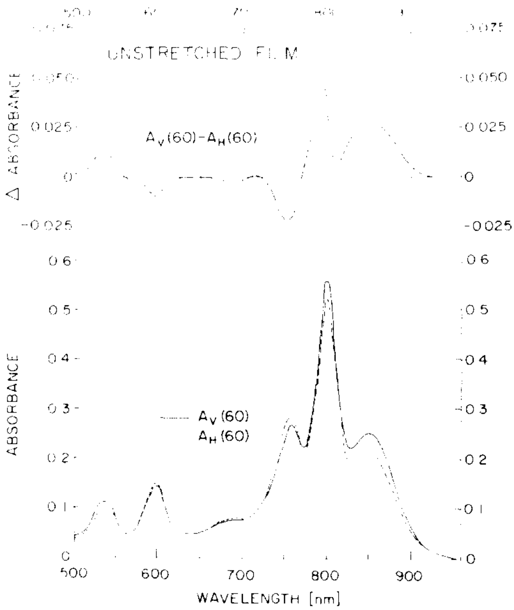

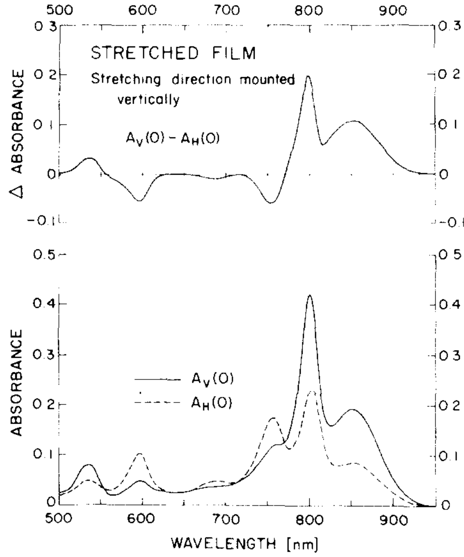

Fig. 2. The polarized absorption and linear dichroism spectra of reaction centers of *Rp. sphaeroides* in an unstretched gelatin film. The angle of incidence of the measuring beam (θ in Fig. 1) was 60°. For vertical polarization the electric vector was parallel to the plane of the film; for horizontal polarization the electric vector made an angle of 60° with the film plane.

Fig. 3. The polarized absorption and linear dichroism spectra of reaction centers of *Rp. sphaeroides* in a stretched gelatin film. The electric vector of the vertically polarized measuring beam was parallel to both the film plane and the stretching direction. The electric vector of the horizontally polarized measuring beam was parallel to the film plane and perpendicular to the stretching direction. The same film section before stretching had been used to obtain the spectra shown in Fig. 2.

value of ϕ, with $n = 1.43$ (1) *, was 37.3°. The electric vector of the measuring beam was vertical for $A_V(60)$ and horizontal (aligned with the x axis inside the film) for $A_H(60)$. Dichroic ratios at the extrema of the linear dichroism spectrum are listed in Table I. Within experimental accuracy, the same ratios were found with other films prepared in the same way. When the film was set normal to the measuring beam ($\theta = 0$), no dichroism was observed; $A_V(0) = A_H(0)$, as expected for random orientation within the plane.

The same film, stretched 2.5 times and mounted with the stretching direction vertical ($\beta = 0$) and with its plane normal to the measuring beam ($\theta = 0$), gave the absorption and linear dichroism spectra shown in Fig. 3, with the electric vector vertical for $A_V(0)$ and horizontal for $A_H(0)$. Dichroic ratios are again listed in Table I. This shows that stretching induced orientation of the reaction centers in the plane of the film.

---

* The refractive index of a stretched film will also be taken as 1.43, the value measured in an unstretched film. Although stretched films appear birefringent when viewed between crossed polarizers, we could detect no significant different between the values of n measured with light polarized parallel and perpendicular to the direction of stretching.

TABLE I

DICHROIC RATIOS OF THE POLARIZED ABSORPTION SPECTRA OF REACTION CENTERS FROM *RHODOPSEUDOMONAS SPHAEROIDES* IN A GELATIN FILM *

The experimental data were obtained using the same film section, before and after stretching. The listed wavelengths are the positions of extrema of the linear dichroism spectra.

Wavelength (nm)	Unstretched film $A_V(60)/A_H(60)$ (Fig. 2)	Stretched film	
		$A_V(0)/A_H(0)$ $\beta = 0°$ (Fig. 3)	$A_H(0)/A_H(60) \cdot K(60)$ $\beta = 0°$ (Fig. 4)
852	1.141 ± 0.012	2.277 ± 0.050	1.031 ± 0.012
798	1.082 ± 0.012	1.920 ± 0.050	1.022 ± 0.012
754	0.929 ± 0.012	0.670 ± 0.050	0.986 ± 0.012
688	0.962 ± 0.025	0.834 ± 0.050	—
597	0.920 ± 0.025	0.480 ± 0.050	—
535	1.102 ± 0.025	1.700 ± 0.100	—

* The experimental error is given as approximate limits for a 95% confidence interval based on three replicate sets of recordings using the same film section.

Tests of axial symmetry in stretched films

According to the model detailed ealier, the transition dipoles of the reaction centers should be aligned with axial symmetry about the axis of stretching. This symmetry is expressed by Eqns. 10 and 11 in that the right side of each equation is independent of θ.

We tested Eqn. 10 by mounting the film section used for Fig. 3 so that the film plane was fixed at several angles θ relative to the measuring beam. The stretching direction was always vertical ($\beta = 0$). The dichroic ratios ($A_V(\theta)/A_H(0)$) were found to be independent of θ within the limits of experimental error as predicted by Eqn. 10 for all angles of θ investigated (0 to 60°).

We also measured the parameters of Eqn. 11, with $\theta = 0$ and 60° and with $K(60°)$ determined through Eqn. 5: $K(60) = A_V(0)/A_V(60)$. The measured spectra of $A_V(0)$ and $A_V(60)$ satisfied Eqn. 5 when $K(60)$ was set at 0.810, in good agreement with the expected value of 0.796 for $\cos\phi$ when $\phi = 37.3°$ (corresponding to $\theta = 60°$ and $n = 1.43$). Results of this test of axial symmetry are shown in Fig. 4. Note that the spectra of $A_H(0)$ and $A_H(60)K(60)$ (with the stretching direction vertical; $\beta = 0$) are nearly identical. The small residual linear dichroism spectrum has superficially the same form as those of Figs. 2 and 3. The dichroic ratios are listed in Table I.

Extrapolation to perfect orientation

As films are stretched to ever greater degrees their linear dichroism spectra reflect a closer approach to the condition of axial symmetry about the stretching axis. The small departure from axial symmetry seen in Fig. 4 is probably a residue of the planar symmetry of an unstretched film; see the comments preceding the derivation of Eqn. 23. The linear dichroism spectrum of Fig. 4 looks like an attenuated version of its counterpart in an unstretched film. But for some purpose we need not concern ourselves with the source of axial asymmetry in a partly stretched film. If strongly stretched films approach a limit of axially symmetric dichroism, we can extrapolate the data from a series of films

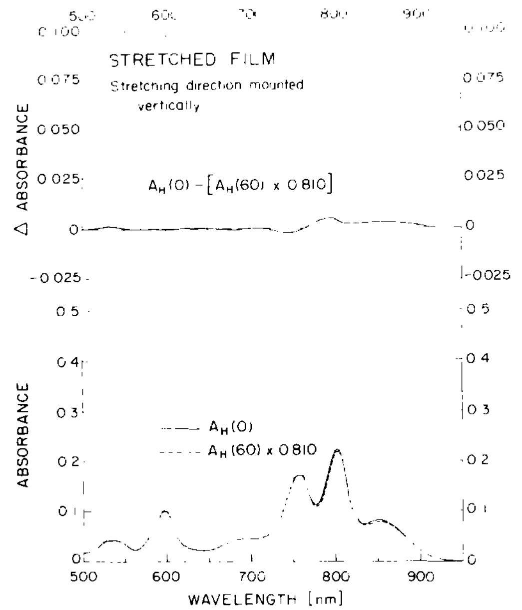

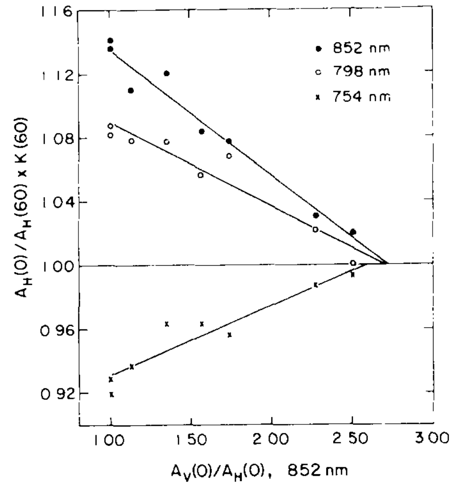

Fig. 4. The polarized absorption and linear dichroism spectra of reaction centers of *Rp. sphaeroides* in a stretched gelatin film, stretching direction vertical. The spectra were recorded using horizontally polarized light, with the film plane fixed at two different angles, 0 and 60°, relative to the electric vector of the measuring beam. In both cases the electric vector was perpendicular to the stretching direction. The factor 0.810 corrects for the difference in path length for the two orientations. The same film gave the spectrum of Fig. 3.

Fig. 5. The relationship between the dichroic ratios $A_H(0)/A_H(60)K(60)$ and $A_V(0)/A_H(0)$ observed in a series of stretched films containing reaction centers (stretching direction vertical). Eight film sections were stretched, each to a different extent. For each film section the dichroic ratios were determined at the wavelengths shown in the Figure.

to that limit. The limit represents perfect axial orientation: $f_2 = 1$, Eqn. 23 reduces to Eqn. 10, and α can be computed from Eqn. 10.

We prepared films stretched to different extents, ranging from 1.0 to 3.0 times, in order to make such an extrapolation. As an analytical framework for the extrapolation, let f_2 be the fraction of reaction centers aligned with the axis of stretching in a given film, with the remainder $1 - f_2$ deployed as in an unstretched film. Then as f_2 ranges from 0 to 1 the dichroic ratios will range monotonically from those of an unstretched film to those of a 'perfectly' stretched film. In particular, with the stretch direction vertical ($\beta = 0$), $A_V(0)/A_H(0)$ ranges from 1 to the maximum value given by Eqn. 10. At the same time, $A_H(0)/A_H(\theta)K(\theta)$ ranges from the value for an unstretched film (Eqn. 14 or 22) down to unity (Eqn. 11). We therefore set each film in the instrument with the stretch direction vertical and measured its spectrum so as to determine $A_V(0)/A_H(0)$ and $A_H(0)/A_H(60)K(60)$ at selected wavelengths. Plots of $A_H(0)/A_H(60)K(60)$ vs. $A_V(0)/A_H(0)$ could then be extrapolated to the limiting case. Such plots are shown in Fig. 5, with $A_V(0)/A_H(0)$ measured at 852 nm and $A_H(0)/A_H(60)K(60)$ measured at three wavelengths. Similar plots were made for these three wavelengths with $A_V(0)/A_H(0)$ expressed at 798, 754, 688, 597 and 535 nm. In all cases the absolute values of $[A_V(0)/A_H(0)]$ were higher in films stretched to a greater extent. For the data in Fig. 5, linear extrapola-

TABLE II

THE DICHROIC RATIOS AND THE ANGLE α FOR THE HYPOTHETICAL CASE OF PERFECT ORIENTATION OF REACTION CENTERS IN A STRETCHED GALATIN FILM *

The listed wavelengths are the positions of extrema of the linear dichroism spectra. The dichroic ratios were obtained by a method described in the text involving extrapolation of experimental dichroic ratios obtained for a series of stretched films. α was calculated from the listed dichroic ratios using Eqn. 10; it is the angle between a transition moment and an axis of symmetry in the reaction center (see the text).

Wavelength (nm)	$A_V(0)/A_H(0)$ $\beta = 0^\circ$		α (deg.)
852	2.68 **	± 0.17	40.8 ± 0.9
798	2.14 **	± 0.12	44.0 ± 0.8
754	0.637 ***	± 0.036	60.6 ± 0.7
688	0.787 ***	± 0.045	57.9 ± 0.8
597	0.403 ***	± 0.058	65.8 ± 1.4
535	1.86 **	± 0.12	46.0 ± 0.9

* The error is given as limits for a 95% confidence interval.

** These ratios were obtained by fitting the experimental data with a straight line.

*** These ratios were obtained by fitting the experimental data with a polynomial of order 2.

tions (least squares fit) converged to a limiting value $A_V(0)/A_H(0) = 2.68 \pm 0.17$ (95% confidence limits) at 852 nm. The results of these extrapolations, together with values of α computed by Eqn. 10 from the limiting values of $A_V(0)/A_H(0)$ are shown in Table II. Note that for some wavelengths the data were better fitted with a quadratic curve rather than a straight line.

The degree of orientation in unstretched films

Having evaluated the angle α by extrapolation with stretched films, we can use Eqn. 22 and the value of $A_V(60)/A_H(60)$ for an unstretched film in order to compute f_1, the oriented fraction of reaction centers in an unstretched film. At 852 nm, α from Table II and $A_V(60)/A_H(60)$ from Fig. 2 and Table I give $f_1 = 0.70 \pm 0.05$ (95% confidence limits). The unstretched film behaves as if 70% of the reaction centers are oriented with their axis of symmetry in the plane of the film, and 30% have random orientation. Using this value of f_1 in Eqn. 22, we can compute α at other wavelengths from the other values of $A_V(60)/A_H(60)$; data of Fig. 2 and Table I. Values of α computed in this way agree with those in Table II. The agreement supports our model for orientation in unstretched films as compared with stretched films *.

Further tests of internal consistency; the degree of orientation in stretched films

Finally, using the value 0.70 that we computed for f_1 in an unstretched film, together with $\alpha = 40.8^\circ$ at 852 nm (Table II), we applied Eqn. 23 to compute f_2, the 'perfectly oriented' fraction of reaction centers in a stretched film. Eqn. 23 was derived by assuming that the residual fraction $1 - f_2$ has the same orientation as in an unstretched film. Taking $A_V(0)/A_H(0) = 2.277$ for a

---

* This agreement is a more refined version of the observation that the linear dichroism spectra of unstretched and stretched films have approximately the same shape.

stretched film measured at 852 nm with $\beta = 0$ (Fig. 3 and Table I), we find $f_2 = 0.845 \pm 0.050$ (95% confidence limits) for the film described in Figs. 3 and 4. With this value of f_2 and the values of $A_V(0)/A_H(0)$ from Fig. 3 and Table I we used Eqn. 23 to compute α at other wavelengths. This treatment using Eqn. 23 was repeated with a slightly stretched film (stretched 1.3 times), for which we obtained $f_2 = 0.131 \pm 0.010$. The sets of values of α computed in these ways again agree with those listed in Table II. For values of f_2 greater than 0.5, the variously computed values of α are also in good agreement if we assume that the residue $1 - f_2$ is oriented at random (Eqn. 18) rather than as in an unstretched film. But with f_2 less than 0.5 the agreement is significantly better with the model implicit in Eqn. 23.

Light-induced absorbance changes

We examined light-induced absorbance changes with polarized light, recording the kinetics of flash-induced changes at successive wavelengths *.

A strongly stretched film was prepared and the 'dark' spectra were measured as before, to obtain $A_V(0)/A_H(0)$ with $\beta = 0$. Then with $\alpha = 40.8°$ at 852 nm (Table II) and $f_1 = 0.70$ (see earlier), we computed $f_2 = 0.94 \pm 0.05$ using Eqn. 23.

We then placed the film in the split-beam spectrometer with $\beta = 0$ (stretch direction vertical) and the plane of the film set 45° from the axes of both the measuring beam and the perpendicular actinic beam ($\theta = 45°$). The measuring beam was polarized with the electric vector either vertical or horizontal, so that we measured $\Delta A_V(45)$ and $\Delta A_H(45)$. The actinic xenon flash (0.1 ms duration) passed through a polarizer so that the electric vector was vertical, aligned with the stretch axis and hence with the axis of symmetry of most of the reaction centers. With this arrangement reaction centers were excited at random, regardless of the excitation wavelength. Artifacts due to photoselection were thereby avoided.

The light-induced changes $\Delta A_V(45)$ and $\Delta A_H(45)$ are plotted against wavelength in Fig. 6. The negative bands at 852, 812 and 600 nm, and the positive band at 790 nm, are attributed to photo-oxidation of the bacteriochlorophyll special pair that acts as photochemical electron donor [1,4], the bands at 852 and 812 nm being identified with Q_y transition moments of the special pair. The inset of Fig. 6 shows that the Q_x absorption of the special pair is also resolved into two components, with bands of different polarizations near 600 and 630 nm. This has not been reported previously.

Dichroic ratios $\Delta A_V(45)/\Delta A_H(45)$ at several wavelengths are listed in Table III. These ratios were fairly uniform from 830 to 880 nm; we averaged the values from 850 to 860 nm for the long wave Q_y transition. Similarly we averaged the values from 595 to 605 nm for the short wave Q_x transition, and 630 to 640 nm for the longer Q_x transition. The low value at 625 can be attributed to overlap with the 600 nm band. At 812 nm the dichroic ratio was about unity, but this value should be interpreted with caution because the change at 812 nm is due partly to blue-shift of the 800 nm band [10] (an

---

* Spectra constructed in this way were more accurate than those obtained [1] by scanning absorbance against wavelength with and without continuous cross-illumination, because they were free from errors due to faulty baseline corrections and secondary changes under prolonged illumination.

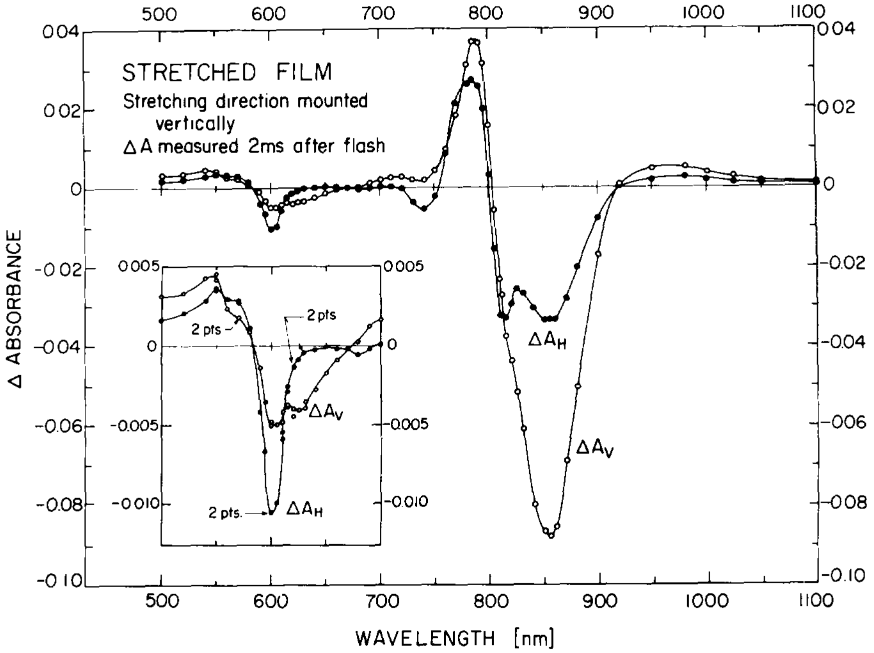

Fig. 6. The polarized light minus dark difference absorption spectra of reaction centers of *Rp. sphaeroides* in a stretched gelatin film. We measured the light-induced absorbance changes in response to a brief actinic flash. The plane of the film was vertical (with the stretching direction vertical) and at 45° to the mutually perpendicular axes of the measuring and actinic beam. Thus the electric vector of the vertically polarized measuring beam was parallel to both the film plane and the stretching direction. The electric vector of the horizontally polarized measuring beam made angles of 45° with the film plane and 90° with the stretching direction. The actinic flash was vertically polarized. We averaged 4 to 8 measurements at each wavelength; replicate absorbance changes were reproducible within 0.001 ΔA (about 1% of the largest changes) and the samples did not deteriorate appreciaiy in the course of several hundred flashes. For measurements above 650 nm the actinic light passed through a blue (Corning 4-96) filter and the photomultiplier was shielded by a red (Corning 2-58) filter. Below 700 nm we used an infrared-insensitive photomultiplier and placed a near infrared (Corning 7-96) filter in the actinic path. The actinic light was saturating with the near infrared filter and gave changes 43% of saturation with the blue filter. The data above 650 nm was normalized to those below 700 nm in the region of overlap, 650—700 nm.

indirect consequence of photooxidation of the special pair), and also overlaps with the 790 and 852 nm bands.

Using these dichroic ratios, with $f_1 = 0.70$ and $f_2 = 0.94$ (see earlier), we applied Eqn. 23 to compute values of α for the transition dipoles associated with these light-induced changes. These are listed in Table III. The value of α near 852 nm agrees well with that obtained from dark spectra, as we expect since this band is almost entirely bleached in the photo-oxidized state. The value of α for the shorter wave Q_x transition of special pair bacteriochlorophyll (600 nm) is close to the value at 597 nm obtained with 'dark' spectra which reflect absorption by all four bacteriochlorophyll molecules in the reaction center. At 630 nm (longer wave Q_x transition of the special pair) we encounter the highest dichroic ratio and correspondingly the smallest angle α between the transition dipole and the axis of symmetry. The value of α at 812 nm should be taken as a crude average of several transition moments.

The 630 nm band is not a peculiarity of reaction centers in gelatin films. It

TABLE III

THE DICHROIC RATIOS AND THE ANGLE α FOR THE POLARIZED LIGHT MINUS DARK DIFFERENCE ABSORPTION SPECTRA SHOWN IN FIG. 6

The listed wavelengths are in the neighborhood of negative bands with minima at 852, 812, 630 and 600 nm. α was calculated from the average value of the selected experimental dichroic ratios using Eqn. 23 for $f_1 = 0.70 \pm 0.05$ and $f_2 = 0.94 \pm 0.05$.

Wsvelength	$\Delta A_V(45)/\Delta A_H(45)$ * $\beta = 0$		α ** (deg.)
850	2.568	average 2.594 ± 0.101	40.3 ± 0.9
855	2.641		
860	2.573		
812	≈1		≈55
640	8.86	average 8.79 ± 1.30	22.5 ± 3.0
630	8.23		
	9.27		
625	4.15		
605	0.499	average 0.495 ± 0.045	64.1 ± 1.1
600	0.486		
	0.459		
595	0.536		

* The error is given as limits for a 95% confidence interval.

** The error is given as limits for a 95% confidence interval and was based on either the uncertainty in the experimental dichroic ratio or the uncertainty in the fraction of oriented reactions centers, whichever was larger.

can be seen also in the light-induced difference spectra of purified reaction centers in solution and in chromatophore membranes.

Discussion

Uniqueness of the model in relation to the data

We have found that a variety of data on the linear dichroism of reaction centers in gelatin films are in excellent accord with the predictions of a simple model. The internal consistency of the data under various manipulations strengthens our confidence in the model and shows the usefulness of the method of Fraser [9] in which the population of reaction centers is decomposed into ideally oriented and unoriented fractions.

Our model states that reaction centers are disposed randomly about an intrinsic axis of symmetry that lies in the plane of an unstretched film and parallel to the axis of stretching in a stretched film. A principal fact supporting this model is the approach to axial symmetry of transition dipoles about the axis of stretching in strongly stretched films. Let us now consider two types of deviation from the strict terms of the model, so as to explore its uniqueness in accounting for the data.

One possibility is that there is a randomly oriented component of reaction centers in a stretched film, aside from the random component $(1 - f_1)$ that is carried along from the unstretched film and is acknowledged in Eqn. 23. We tested this possibility by introducing a new, additional random fraction into the equations for stretched films. When this fraction reached 10% of the total, the computed value of α for the absorbance change at 630—640 nm (Table III) fell from 22.5° to zero, and greater fractions led to imaginary values for sinα. We thus set a limit of '10% random' on this kind of departure from our model.

Second, the axis of symmetry of each reaction center could make a specific angle (other than zero) with the stretching axis, or with the plane of an unstretched film. Then if the reaction centers were oriented randomly about their own axes of symmetry, a stretched film would continue to show axial symmetry. We analyzed this possibility, and concluded that a computed value of α (the average angle between a transition dipole and the axis of stretching) will always be greater than δ, the angle between the axis of symmetry of the reaction center and the axis of stretching. The value of 22.5° for α at 630 nm (Table III) thus sets an upper limit for δ. The 'true' value of α (angle between transition moment and axis of symmetry) is then within 5% of the computed value for $\alpha > 40°$, but for $\alpha = 22.5°$ the true value could be anything between 0 and 22.5°.

Having explored these variations, we accept our model as a useful framework for interpreting our data.

The structure of gelatin

The model is compatible with what is known about the structure of gelatin. Gelatin is denatured collagen. Gelation is thought to involve partial renaturation of tropocollagen (a superhelix formed from three polypeptides with interchain hydrogen bonding) and the creation of an amorphous gel network by random binding between macromolecules [11]. X-ray diffraction [12] shows that dehydration causes the superhelices to lie with their long axes in the plane of a dried film, oriented randomly within the plane. Partial rehydration followed by stretching then aligns the superhelices along the axis of stretching, as indicated by measurements of linear dichroism in the infrared [13]. The axis of tropocollagen thus has the same orientation as the hypothetical axis of symmetry of the reaction center.

Correlation with transition moments of chromophores in the reaction center

Having obtained a set of characteristic angles α for the directions of transition dipoles in the reaction center, we wish to associate these, as far as possible, with transition moments of the component chromophores.

In light minus dark spectra the bands at 852 and 812 nm * have been identified with the special pair of bacteriochlorophyll molecules that acts as photochemical electron donor, the bands arising from exciton interaction (dipole coupling) of the Q_y transitions of the component monomers. We have now found the expected 'Q_x' counterparts at 630 and 600 nm. The band at 812 nm is not resolved from other light-induced changes, but at 852, 630 and 600 nm the changes can be identified mainly with single transition moments of the special pair. Dichroic ratios are uniform over the greater (spectrally resolved) parts of these bands. Excitation of the 852 (or 870) nm transition gives a polarization value of +0.45, close to the theoretical maximum of +0.5 for a

---

* Reported previously as 850—870 nm and 805—812 nm as observed under different conditions [1,2,6, 10].

single transition, throughout this band, in photoselection experiments (10) * and in measurements of polarized fluorescence [14].

The properties of these four bands of the special pair bacteriochlorophyll are consistent with a simple application of molecular exciton theory [15—17] to a dimer. The geometry of the dimer is suggested by the relative integrated intensities of the absorption bands, with the 852 nm band far more intense than the 812 nm band, and the 600 nm band far more intense than the 630 nm band. Thus in the Q_y region the transition of lower energy is favored, and conversely in the Q_x region. Exciton theory then implies that the Q_y transition moments of the component monomers are roughly parallel (within 40°) and predominantly collinear, while the monomeric Q_x transition moments are roughly parallel and predominantly side by side.

A simple application of exciton theory for a dimer can thus account for the observed splitting and relative intensities of the absorption bands, for the available data on circular dichroism, and for the conclusion of Vermeglio et al. [10] that Q_x (600 nm) is nearly perpendicular to Q_y (852 nm). It also predicts Q_x (630 nm) $\perp$ Q_x (600 nm) and Q_y (812 nm) $\perp$ Q_y (852 nm).

While the foregoing description in terms of exciton interactions appears satisfactory, we can easily imagine other possibilities. For example, the 812 nm band could result from exciton interaction between the special pair and the 800 nm component of bacteriochlorophyll. The disruption of this interaction, when the special pair is photo-oxidized, could account for the bleaching of the 812 nm band.

A similar argument could be made about the origin of the 630 nm band. Thus we should be cautious in identifying these transitions with specific chromophoric interactions, even though the 'special pair dimer' treatment is appealingly direct and seems sufficient.

In absorption spectra such as those in Fig. 2—4, most of the bands contain contributions from two or more of the six tetrapyrroles in the reaction center. Some of the bands can be assigned with reasonable certainty. The 852 nm band represents a Q_y transition of the bacteriochlorophyll special pair; it is the same as its counterpart in the light minus dark difference spectrum, which is fully bleached in strong light. The band near 535 nm represents the Q_x transitions of the two molecules of bacteriopheopytin in the reaction center. At low temperature the 535 nm band is split into two bands near 532 and 545 nm [1]. Dicrhoic ratios are uniform across these bands at low temperature, and approximately equal to that across the 535 nm band at room temperature. The angle α computed at 535 nm therefore applies to both components. The two components are not parallel to each other [10]. They probably do not arise from exciton splitting in a dimer, because circular dichroism spectra do not show bands of opposite sign in either the 535 nm (Q_x) or the 754 nm (Q_y) regions of bacteriopheophytin absorption [18,19]. Also the 754 nm band is not split, in absorption or in linear dichroism spectra [1,4]. A stronger argument against exciton coupling of the bacteriopheophytins is that the formation of the earliest photoproduct p^f or '$p^+ \cdot I^-$' is attended by bleaching of the 545

---

* Vermeglio et al. [10] have shown that reports of lower polarization values, +0.25 [21,22] were in error due to the unsuspected presence of a mixed polulation of reaction centers with different reaction kinetics.

nm band and no change of the 530 nm band [20]. In the coupled case the obliteration of one of these bands should cause a marked perturbation of the other. We therefore assume that the two components near 535 nm represent two molecules of bacteriopheophytin in different environments. This assumption also gives a better fit to photoselection data of Vermeglio et al. [10] than does the assumption of exciton coupling. We conclude that the Q_x transition moment of each bacteriopheophytin molecule makes an angle $\alpha = 46°$ with the axis of symmetry, and that the value at 754 nm, 61°, is for the sum of the independent Q_y transition moments.

Acknowledgements

This work was supported by Contract No. E(11-1)-3162 with the U.S. Department of Energy and Grant No. PCM76-01556 from the National Science Foundation.

References

1 Rafferty, C.N. and Clayton, R.K. (1978) Biochim. Biophys. Acta 502, 51—60
2 Straley, S.C., Parson, W.W., Mauzerall, D.C. and Clayton, R.K. (1973) Biochim. Biophys. Acta 305, 597—609
3 Norris, J.R., Uphaus, R.A., Crespi, H.L. and Katz, J.J. (1971) Proc. Natl. Acad. Sci. U.S. 68, 625—628
4 Vermeglio, A. and Clayton, R.K. (1976) Biochim. Biophys. Acta 449, 500—515
5 Clayton, R.K. (1960) Biochim. Biophys. Acta 37, 503—512
6 Clayton, R.K. and Wang, R.T. (1971) Methods Enzymol. 23, 696—704
7 Clayton, R.K. (1971) Light and Living Matter, Vol. 2, Appendix C, McGraw-Hill, N.Y.
8 Cherry, R.J., Hsu, K. and Chapman, J.D. (1972) Biochim. Biophys. Acta 267, 512—522
9 Fraser, R.D.B. (1953) J. Chem. Phys. 21, 1511—1515
10 Vermeglio, A., Breton, J., Paillotin, G., and Cogdell, R.J. (1978) Biochim. Biophys. Acta 501, 514—530
11 Veis, A. (1964) The Macromolecular Chemistry of Gelatin, Academic Press, New York, N.Y., pp. 267—275
12 Bradbury, E. and Martin, C. (1952) Proc. R. Soc. A214, 183—192
13 Ambrose, E.J. and Elliot, A. (1951) Proc. R. Soc. A206, 206—219
14 Ebrey, T.G. and Clayton, R.K. (1969) Photochem. Photobiol. 10, 109—117
15 Kasha, M. (1963) Radiation Research 20, 55—71
16 Kasha, M., Rawls, H.R. and El-Bayoumi, M.A. (1965) Pure Appl. Chem. 11, 371—392
17 Tinoco, I., Jr. (1963) Rad. Res. 20, 133—139
18 Sauer, K., Dratz, E.A. and Coyne, L. (1968) Proc. Natl. Acad. Sci. U.S. 61, 17—24
19 Reed, D.W. and Ke, B. (1973) J. Biol. Chem. 248, 3041—3045
20 Rockley, M.G., Windsor, M.W., Cogdell, R.J. and Parson, W.W. (1975) Proc. Natl. Acad. Sci. U.S. 72, 2251—2255
21 Mar, T. and Gingras, G. (1976) Biochim. Biophys. Acta 440, 609—621
22 Shuvalov, V.A., Asadov, A.A. and Krakhmaleva, I.N. (1977) FEBS Lett. 76, 240—245